A Time-Domain Grey-Box System Identification Procedure for Scale Model Helicopters

Wei Yuan and Jay Katupitiya
School of Mechanical and Manufacturing Engineering
The University of New South Wales, Sydney NSW 2052, Australia
Email: {w.yuan, J.Katupitiya}@unsw.edu.au

***Abstract*—This paper is about a time-domain grey-box system identification applicable to scale model helicopters. It presents a unique way to obtain the initial values to be used in the estimation process and a systematic way to partition the set of state equations and to identify all its parameters. A widely published linearized model suitable for hover and near hover condition is used in this paper. There is no need to go through tedious experiments to determine good initial parameter values to start estimation. The performance of the proposed procedure is demonstrated using a ground-truth model and by showing the well-matched outputs and system eigenvalues, as well as the convergence of the identified parameters to their true values. The validation using real flight data is further strengthened by showing the prediction results.**

I. Introduction

The R&D into UAVs have achieved significant progresses in the last few decades. Among these, scale model helicopters are particularly attractive as they provide excellent platforms to gather flight data and to develop control methodologies. Unlike fixed wing aircraft, scale-model helicopters are attractive due to their ability to operate in many manoeuvering modes such as hovering, vertical takeoff-landing, low-speed cruise, pirouette, etc. The helicopters have significantly more complex flight dynamics and as a result complex dynamic models. They are naturally unstable, nonlinear, highly coupled and multiple-input multiple-output (MIMO) system. However, the helicopters can be considered as a LTI MIMO system in hover and low-speed cruise modes where the most meaningful applications, such as navigation and surveillance, are carried out. To be able to design high quality flight controllers for hover and low-speed cruise, it is necessary to obtain a sufficiently accurate LTI MOMO dynamic model of the helicopter.

In general, two modeling approaches are widely used to obtain dynamic models of helicopters. They are first-principle modeling and modeling through system identification. The first-principle modeling is based on physical understanding of the helicopter's dynamics. The resulting mathematical equations are typically nonlinear and have dozens of unknown physical parameters that need to be determined. In order to get accurate parameters, numerous measurements and experiments with extreme care are required [1].

Compared to the first-principle modeling, system identification modeling uses real flight data to obtain the actual helicopter dynamics. This approach, especially the grey-box system identification method, has become a popular way to obtain accurate and practical LTI MIMO parametric helicopter models for flight control design. In Shim's PhD thesis [2], he identified a LTI MIMO state space model for a helicopter. Based on the identified model, a way point navigation control system was successfully implemented. Cai et al [3] identified the unknown parameters in the LTI MIMO helicopter model using real flight data and developed a position control in hovering condition. Although the model is a linear model in hovering and near-hovering flight conditions, Peng and Cai *et al* [4] have applied this linear model to realize an autonomous flight controller, which consists of tasks including automatic takeoff & landing, hovering, slithering, pirouetting and spiral turning, etc. Garratt *et al* [5] used the grey-box system identification method to model two different sizes of scale model helicopters for designing automatic landing control system.

To our knowledge, the most used grey-box system identification tools for scale-model helicopters are the prediction error method (PEM) in MATLAB® System Identification Toolbox® [6] and the software package CIFER®(Comprehensive Identification from Frequency Responses) [7]. Both can be generally summarized as a parametric estimation problem, the aim of which is to find values of unknown model parameters λ in a mathematically derived helicopter model, using flight data. The helicopter model is formulated as a MIMO state space model which mathematically describes the helicopter dynamics. The unknown parameters λ in the model are iteratively determined by minimizing a cost function $J(\lambda)$.

Both methods start minimizing the cost function $J(\lambda)$ from a set of initial values λ_0 of the model parameters. In order to get an accurate estimation, the values of λ_0 must be not too far from the real values of the model parameters P [7], [6]. Mettler [8], [9], [10], Cai [3] and Garratt [5] did not present in detail how they obtained the initial values to start the parameter estimation. Lorenz [11] and Shim [2] used initial guesses to start the identification in their papers, however, the estimation can easily converge to a local minimum of the cost function $J(\lambda)$ or even diverge [2]. One popular and reliable way to obtain good initial values is based on the first-principle modeling [12], [13] and [7]. As mentioned above, numerous experiments and measurements are needed to get these parameters and it is too cumbersome and time consuming.

An alternative grey-box system identification toolbox, SIDPAC (System Identification Programs for Aircraft) [14], written in MATLAB®, is used here to identify a LTI MIMO state space model with 13 states for a scale-model helicopter. SIDPAC uses output-error method (OEM) to estimate the unknown parameters in a LTI MIMO aircraft model. Theoretically it still needs suitable initial parameter values to reach the global minimum of the cost function [14], [15]. The toolbox also provides equation-error method (EEM) to obtain initial values but only in some equations where the states and their derivatives and also the inputs are all available.

As unmeasurable states exist in some subsystems of our helicopter model, the constraint on the sign of the key parameters are used to start the OEM. The correct sign constraints are all based on the physical meanings of all the key parameters.

II. Hover model of scale-model helicopter

As mentioned above, the scale model helicopter is a nonlinear, naturally unstable, highly coupled and multiple-input-multiple-output system, but the hover dynamics can be linearized as a LTI MIMO state space model at the trimmed point. The model structure used in this paper is based on Mettler's work on the identification of helicopter models [8], [9]. This model is suitable and has been used widely to implement flight control systems, e.g. [3], [2]. The linearized model for hover is given by,

$$\dot{x} = Ax + Bu \quad \text{and} \tag{1}$$

$$y = Cx, \tag{2}$$

where $x = [u\ v\ p\ q\ \Phi\ \Theta\ a\ b\ w\ r\ r_{fb}]^T$ is the state vector with u, v, w as the longitudinal, lateral and vertical velocities, respectively; p, q, r as the roll, pitch and yaw rates, respectively; a, b as the longitudinal and lateral flapping angles, respectively with Φ and Θ as roll and pitch angles, respectively. The control input, or the stick inputs is $u = [\delta_{lat}\ \delta_{lon}\ \delta_{col}\ \delta_{ped}]^T$ where the elements in the order are: roll rate control, pitch rate control, collective pitch control and the yaw rate control. The output vector is, $y = [u\ v\ w\ p\ q\ r\ \Phi\ \Theta]^T$. The matrices A and B in (1) are:

$$A = \begin{bmatrix} X_u & 0 & 0 & 0 & 0 & -g & -g & 0 & 0 & 0 & 0 \\ 0 & Y_v & 0 & 0 & g & 0 & 0 & g & 0 & 0 & 0 \\ L_u & L_v & 0 & 0 & 0 & 0 & L_a & L_b & 0 & 0 & 0 \\ M_u & M_v & 0 & 0 & 0 & 0 & M_a & M_b & 0 & 0 & 0 \\ 0 & 0 & 1 & 0 & 0 & 0 & 0 & 0 & 0 & 0 & 0 \\ 0 & 0 & 0 & 1 & 0 & 0 & 0 & 0 & 0 & 0 & 0 \\ 0 & 0 & 0 & -1 & 0 & 0 & \frac{-1}{\tau_a} & A_b & 0 & 0 & 0 \\ 0 & 0 & -1 & 0 & 0 & 0 & B_a & \frac{-1}{\tau_a} & 0 & 0 & 0 \\ 0 & 0 & 0 & 0 & 0 & 0 & Z_a & Z_b & Z_w & Z_r & 0 \\ 0 & 0 & N_p & 0 & 0 & 0 & 0 & 0 & N_w & N_r & N_{rf} \\ 0 & 0 & 0 & 0 & 0 & 0 & 0 & 0 & 0 & K_r & K_{rf} \end{bmatrix} \tag{3}$$

$$B = \begin{bmatrix} 0 & 0 & 0 & 0 \\ 0 & 0 & 0 & 0 \\ 0 & 0 & 0 & 0 \\ 0 & 0 & 0 & 0 \\ 0 & 0 & 0 & 0 \\ 0 & 0 & 0 & 0 \\ A_{lat} & A_{lon} & 0 & 0 \\ B_{lat} & B_{lon} & 0 & 0 \\ 0 & 0 & Z_{col} & 0 \\ 0 & 0 & N_{col} & N_{ped} \\ 0 & 0 & 0 & 0 \end{bmatrix}. \tag{4}$$

In the matrices A and B, there are more than 30 unknown parameters to be identified. It is impractical to estimate all the parameters in one go. So a partitioned system identification procedure based on the reliable flight test steps is used to identify subsystems in a partitioned way.

III. Initial Values

Almost all the grey-box system identification work reported in the literature express the same concern, i.e., the estimation should start from a good set of initial values λ_0 which can converge to the global minimum of the cost function [15], [14], [16] and [7], in other words, those grey-box identification algorithms, as well as the OEM method used in this paper, cannot work properly without such a set of initial values.

Our aim is to work out a practical and efficient method to find suitable initial values directly from flight data without tedious white-box modeling or blind initial guesses. The basic idea is as follows: First, the physical meanings of the key parameters in each subsystem are examined. It provides important information to constrain the estimation ranges of parameters and avoid calculating the cost function in some parameter ranges where no physical meaning exists. Second, the EEM is used in some equations to obtain suitable initial values from measured and input data. After obtaining all the *a priori* information mentioned above, the OEM can start a reliable parameter estimation.

A brief introduction of the OEM and EEM in SIDPAC is given below.

IV. Estimation Algorithms

SIDPAC has been successfully used at NASA Langley Research Center with data from many different flight test programs and wind tunnel experiments [17]. A brief presentation of the two parameter estimation processes is given below.

A. Output-Error Method

OEM is one of the most used maximum likelihood parameter estimation methods for LTI MIMO aircraft dynamic system. The goal of the OEM is to minimize the cost function by tuning the model parameter λ:

$$J(\lambda) = \frac{1}{N}\sum_{i=1}^{N} \mathcal{V}(i)\hat{\mathcal{R}}^{-1}\mathcal{V}^T(i), \tag{5}$$

where $\mathcal{V}(i)$ is the output error between model output $y(i)$ and measured output $z(i)$

$$\mathcal{V}(i) \quad = \quad z(i) - y(i) \qquad i = 1, 2, ..., N \tag{6}$$

and $\hat{\mathcal{R}}$ is the output error covariance matrix.

B. Equation-Error Method

In some rows in the state-space model, the related states, in addition to the inputs, are all measured. The state derivatives there are either measured or can be found from numerical differentiation. In this case, the unknown parameters in these equations can be estimated using the EEM without any starting value. This can be generalized in the form of the following equation:

$$\dot{x} = \sum_{j=1}^{n} \lambda_j^a x_j + \sum_{j=1}^{n} \lambda_j^b u_j \tag{7}$$

and the cost function to be minimized is

$$J(\lambda^{a,b}) = \frac{1}{2} \sum_{i=1}^{N} \mathcal{E}(i)^T \mathcal{R}^{-1} \mathcal{E}(i), \tag{8}$$

where $\mathcal{E}(i)$ is the equation error

$$\mathcal{E}(i) = \dot{x} - \sum_{j=1}^{n} \hat{\lambda}_j^a x_j - \sum_{j=1}^{n} \hat{\lambda}_j^b u_j \qquad \text{i = 1,2,...,N} \tag{9}$$

and $\mathcal{R}$ is the equation error covariance matrix.

More details about SIDPAC and its OEM and EEM methods can be found in [14].

C. Partitioned System identification Procedure

The partitioned systems include lateral translational dynamics, roll dynamics, longitudinal translational dynamics, pitch dynamics, heave dynamics and yaw dynamics. Mettler suggested an identification process in [9], but we made some changes to suit our own procedure. The biggest difference is that before identifying roll dynamics the lateral translational dynamics needs to be identified so that the translational effect can be considered into roll dynamics identification. It is the same for identification of longitudinal translational dynamics and pitch dynamics.

The cross coupling effects among these subsystems cannot be covered in the partitioned systems. However, they are not the dominant parameters that capture the main dynamics of each subsystem. These parameters can be identified in coupled systems after obtaining the dominant parameters. Even the dominant parameters will be further refined at the final step.

1) Lateral translational dynamics:

$$\dot{v} = Y_v v + g\Phi + gb \tag{10}$$

Y_v is the speed force damping derivative in y-direction, physically should be a negative value. g is known as 32.2 ft/s^2.

When exciting the helicopter with low frequency lateral input, the flapping dynamics is ignorable, i.e. , the term gb in (10) can be ignored. So the only parameter to be identified here is Y_v.

In the equation, v and Φ are the collected flight data and $\dot{v}$ can be derived from the data set v. The EEM is used to estimate the parameter Y_v. This method does not need any initial value.

2) Roll dynamics:

$$\begin{bmatrix} \dot{v} \\ \dot{p} \\ \dot{\Phi} \\ \dot{b} \end{bmatrix} = \begin{bmatrix} Y_v & 0 & g & g \\ L_v & 0 & 0 & L_b \\ 0 & 1 & 0 & 0 \\ 0 & -1 & 0 & -1/\tau_a \end{bmatrix} \begin{bmatrix} v \\ p \\ \Phi \\ b \end{bmatrix} + \begin{bmatrix} 0 \\ 0 \\ 0 \\ B_{lat} \end{bmatrix} \delta_{lat} \tag{11}$$

Here, L_b represents the roll rotor spring coefficient and should have a positive sign. L_v describes how the helicopter's roll dynamics responses to an increase in v. As a wind gust from left side causes a positive rolling motion, L_v has a positive sign. B_{lat} is the gain from the lateral input to the roll dynamics with a positive sign. τ_a is the time constant that is due to the stabilizer bar, Shim shows in [2] that the time constant τ_a expressed in seconds can be roughly calculated with,

$$\tau_a = \frac{5}{\Omega_R/60}, \tag{12}$$

where Ω_R is the main rotor speed expressed in rpm. For this helicopter, τ_{a0} = 0.3333. This value will be used as the initial estimate of τ_a. As the main rotor speed is not strictly constant in hover mode, a loose range of [0.3τ_{a0}, 1.2τ_{a0}] is put as its constraint.

The output data p and v and the input signal δ_{lat} are used in the OEM to estimate the unknown parameters L_v, L_b, τ_a and B_{lat} with their constraints.

3) Longitudinal translational dynamics:

$$\dot{u} = X_u u - g\Theta - ga \tag{13}$$

X_u is the speed force damping derivative in x-direction, physically should be a negative value. Similar to (10), it is the only parameter to be estimated using the EEM with low frequency longitudinal input.

4) Pitch dynamics:

$$\begin{bmatrix} \dot{u} \\ \dot{q} \\ \dot{\Theta} \\ \dot{a} \end{bmatrix} = \begin{bmatrix} X_u & 0 & -g & -g \\ M_u & 0 & 0 & M_a \\ 0 & 1 & 0 & 0 \\ 0 & -1 & 0 & -1/\tau_a \end{bmatrix} \begin{bmatrix} u \\ q \\ \Theta \\ a \end{bmatrix} + \begin{bmatrix} 0 \\ 0 \\ 0 \\ A_{lon} \end{bmatrix} \delta_{lon} \tag{14}$$

M_a is the pitch rotor spring coefficient and should be positive. M_u describes how the helicopter's pitch dynamics responses to an increase in u. If the helicopter experiences a wind gust from back, it has a negative pitching motion. So M_u has a negative value. A_{lon} is the gain from the longitudinal input to the pitch dynamics and is a negative quantity.

Similar to the estimation of roll dynamics, the output data q and u and the input signal δ_{lon} are used to estimate the unknown parameters M_u, M_a, τ_a and A_{lon} with their constraints.

5) Coupled longitudinal and lateral dynamics:

$$\begin{bmatrix} \dot{u} \\ \dot{v} \\ \dot{p} \\ \dot{q} \\ \dot{\Phi} \\ \dot{\Theta} \\ \dot{a} \\ \dot{b} \end{bmatrix} = \begin{bmatrix} X_u & 0 & 0 & 0 & 0 & -g & -g & 0 \\ 0 & Y_v & 0 & 0 & g & 0 & 0 & g \\ L_u & L_v & 0 & 0 & 0 & 0 & L_a & L_b \\ M_u & M_v & 0 & 0 & 0 & 0 & M_a & M_b \\ 0 & 0 & 1 & 0 & 0 & 0 & 0 & 0 \\ 0 & 0 & 0 & 1 & 0 & 0 & 0 & 0 \\ 0 & 0 & 0 & -1 & 0 & 0 & -1/\tau_a & A_b \\ 0 & 0 & -1 & 0 & 0 & 0 & B_a & -1/\tau_a \end{bmatrix} \begin{bmatrix} u \\ v \\ p \\ q \\ \Phi \\ \Theta \\ a \\ b \end{bmatrix} + \begin{bmatrix} 0 & 0 \\ 0 & 0 \\ 0 & 0 \\ 0 & 0 \\ 0 & 0 \\ 0 & 0 \\ A_{lat} & A_{lon} \\ B_{lat} & B_{lon} \end{bmatrix} \begin{bmatrix} \delta_{lat} \\ \delta_{lon} \end{bmatrix} \tag{15}$$

The two subsystems (11) and (14) are combined to form the coupled longitudinal-lateral model (15) and the cross-coupling parameters L_a, M_b, A_b, B_a, L_u, M_v, A_{lat} and B_{lon} can be estimated with OEM using a flight data set which are excited by two inputs δ_{lat} and δ_{lon} together. The estimation doesn't require any specific initial values but 0 for all these 8 parameters. The identified parameters from earlier steps 1) to 4) are to be refined at this step simultaneously.

6) Heave dynamics:

$$\dot{w} = Z_a a + Z_b b + Z_w w + Z_r r + Z_{col}\delta_{col} \tag{16}$$

Z_a and Z_b describe the cross coupling effects from flapping dynamics to heave channel. And Z_r describes the effect from yaw rate changes. As the main concern is the vertical response to the collective input and the data set of $\dot{w}$, w and δ_{col} are used to estimate the heave dynamics, the terms $Z_a a$, $Z_b b$ and $Z_r r$ will drop out of the above equation. Once this approximation is made, the parameters Z_w and Z_{col} can be obtained via the EEM, requiring no initial values. Z_w represents the heave damping with a negative value. Z_{col} is the gain from the collective input to the heave dynamics and is a negative quantity.

7) Yaw dynamics:

$$\begin{bmatrix} \dot{r} \\ \dot{r}_{fb} \end{bmatrix} = \begin{bmatrix} N_r & N_{rf} \\ K_r & K_{rf} \end{bmatrix} \begin{bmatrix} r \\ r_{fb} \end{bmatrix} + \begin{bmatrix} N_{ped} \\ 0 \end{bmatrix} \delta_{ped} \tag{17}$$

N_r represents the yaw damping coefficient with a negative value. N_{ped} is the gain from the yaw rate control input to the yaw dynamics and is a positive quantity. As a feedback yaw rate gyro is installed on the helicopter, the yaw rate feedback r_{fb} provides negative yaw rate compensation to enhance the yaw stability. K_r is the yaw rate feedback gain and is a positive value. Additionally, two constraints are added between the parameters to enable successful identification at this step [9]:

$$N_{rf} = -N_{ped} \tag{18}$$

$$K_{rf} = 2N_r \tag{19}$$

Taking all the constraints just mentioned above, the OEM is to estimate the unknown parameters N_r, N_{ped}, K_r, N_{rf} and K_{rf} by using the measured yaw rate r and the yaw rate control signal δ_{ped} to.

8) Coupled heave and yaw dynamics:

$$\begin{bmatrix} \dot{w} \\ \dot{r} \\ \dot{r}_{fb} \end{bmatrix} = \begin{bmatrix} Z_w & Z_r & 0 \\ N_w & N_r & N_{rf} \\ 0 & K_r & K_{rf} \end{bmatrix} \begin{bmatrix} w \\ r \\ r_{fb} \end{bmatrix} + \begin{bmatrix} Z_{col} & 0 \\ N_{col} & N_{ped} \\ 0 & 0 \end{bmatrix} \begin{bmatrix} \delta_{col} \\ \delta_{ped} \end{bmatrix} \tag{20}$$

Two heave-to-yaw coupling parameters (N_w and N_{col}) and one yaw-to-heave coupling parameter (Z_r) are to be estimated at this step using a set of data with two inputs, δ_{col} and δ_{ped}. The OEM is used with initial values of both parameters set to zero.

9) Complete dynamic equation: The coupled longitudinal-lateral model in (15) and the coupled heave-yaw model in (20) are combined as the complete model structure (1) with two further cross-coupling parameters Z_b and N_p. The parameter Z_a is fixed to 0, because its original value in the "true" plant was set to 0.

All the input data (δ_{lat}, δ_{lon}, δ_{col}, δ_{ped}) and output data (u, v, w, p, q, r Φ, Θ) are used in the OEM with Z_{b0}=0 and N_{p0}=0 to run the final estimation.

The final step of the entire estimation procedure is to refine all the parameters determined with a new set of flight data using the OEM with the so far determined parameter values as the starting values.

V. Results in Simulations

In order to prove and validate our preliminary method at this stage, a simulation model is used to generate hover flight data for the system identification. As Shim provided a clear and reproducible LTI MIMO model for a Yamaha R-50 helicopter in [2], this model is considered here as the "true" helicopter which is trimmed and flies with a quasi-constant rotor speed of 900 RPM in hover mode. Although the model simplifies the real situation, it describes the hover dynamics, which is dominant in low frequency, well. As the measurement bias and high frequency noise are very common in real life situation, the flight data generated from this model is substantially corrupted with certain Gaussian white noises and constant biases,

$$\dot{x} = Ax + Bu \quad \text{and} \tag{21}$$

$$y = Cx + Nw + Gd, \tag{22}$$

where w is the measurement noises and d the measurement biases. The matrices N and G are diagonal matrices with weights along the diagonal that can be adjusted to add noise and bias.

The positive directions of the helicopter coordinate and controller inputs are shown in Fig. 1. They are of importance to understand the correct motions from recorded flight data. According to the definition, the signs of the control derivatives in matrix B and the key derivatives in matrix A can be determined by combining their physical meanings and the flight motions. Details are described in the next section.

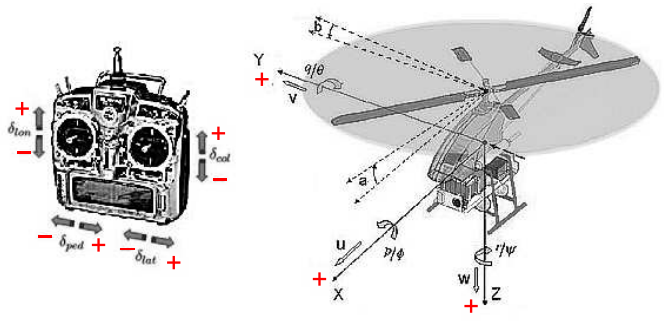

Fig. 1. Definition of coordinate and controller inputs (modified from [18])

.

The parameter values in the real model are listed in column "real " value in Table I. The acceleration due to gravity g is a known parameter and is set at 32.2 ft/s^2. Notice that Shim used imperial units in his original work, but he didn't clearly indicate the unit of each parameter listed in the column. In order to avoid incorrect converting, we keep the original units in this example.

The comparison of the convergence with and without the sign constraints in the identification procedure is presented first. Here is an example at step 2) for estimating B_{lat}. The Estimation runs from the starting value 0 with and without the sign constraints. From Fig.2, we can see that the correct sign gives a necessary constraint to avoid stepping into a wrong range. In contrast to that, the original OEM method, which doesn't combine with the sign constraint, cannot return a correct estimate starting from the same initial value, 0. In this case, it must either have further initial guesses or find a better initial value to get the estimation done.

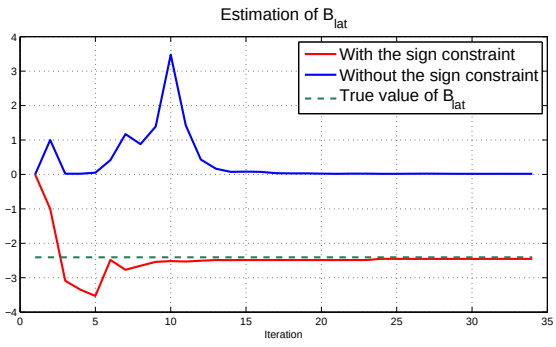

Fig. 2. An example of proper convergence with correct sign constraint.

Figure 3, 4 and 5 compare the responses of the identified system to the "true" system responses. Also note that the outputs of the "true" system have been corrupted by noise and bias before using the flight data in the estimation process. Under these circumstances, the identified model shows an excellent agreement in each channel. The precision of the model in each channel can be quantified by "fit" value [16]:

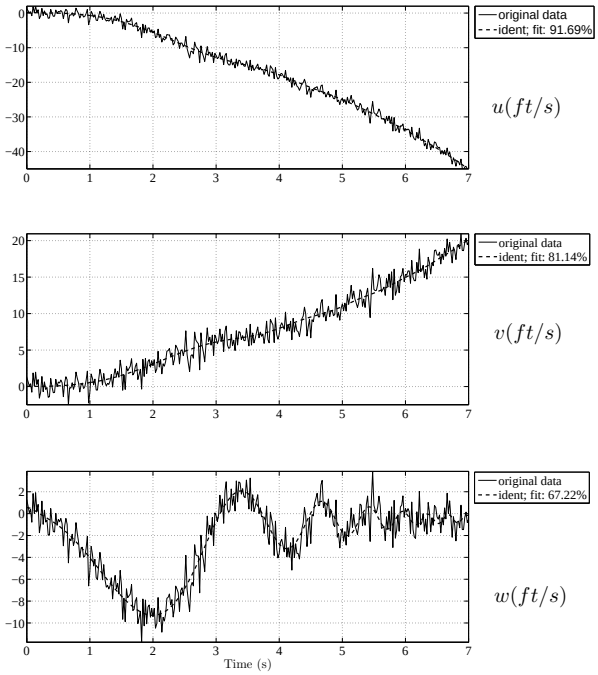

Fig. 3. Identification results for u, v and w.

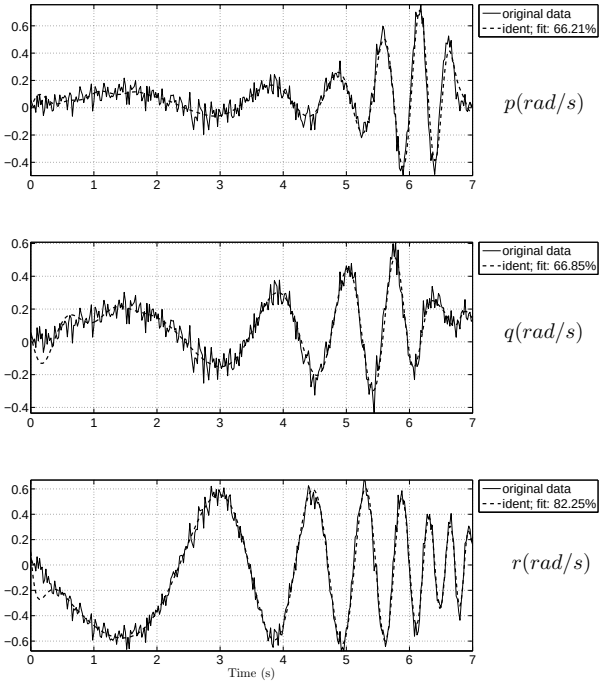

Fig. 4. Identification results for p, q and r.

$$fit = 100 \times (1 - \frac{\sqrt{(y-z)^2}}{\sqrt{(z-\overline{z})^2}}) \quad (23)$$

where y is the output of the identified model and z is the output of the real system. And $\overline{z}$ is the mean value of z.

Although it is popular to use Cramer Rao Bound(CR%)

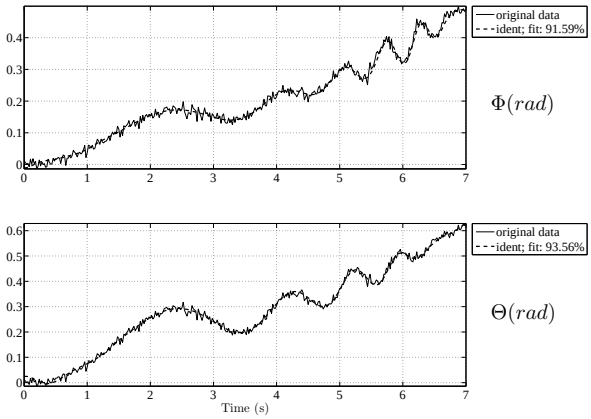

Fig. 5. Identification results for Φ and Θ (rad).

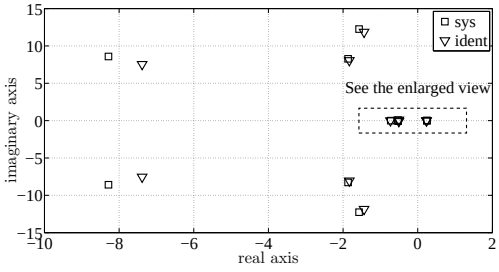

Fig. 6. Eigenvalues.

and Insensitivity (I%) [9], [7] or standard error [19], [17] to indicate the estimation accuracy, these statistics describe the estimation itself but cannot indicate the difference between the estimates and the true values, especially when the true vales are not available. As the "true" parameters of the plant is known in this simulation example, it's more reasonable to compare the identified values to the real model parameters. The mean values of the identified parameters are listed in Table.I. Although the parameter estimation has reached a good accuracy level, it's still not intuitive to assess the accuracy of the identification. For that, the eigenvalues of the original model and the identified one are given in Fig.6. The eigenvalues of the identified model are all close to the original ones, which means the model is capable to describe the characteristics of the system. The time-domain prediction ability of the identified model will verify it further.

To validate the prediction performance of the identified model, the model was excited with the control input data from another set of flight data which was not used in the identification process. The predicted helicopter responses are compared with the "real" outputs. The comparison of linear velocities (u, v, w), angular rates (p, q, r) and two angles (Φ, Θ) is shown in Fig. 8 - 10. The model is excited at time 1.0 (sec) and it shows an excellent agreement with the original system for all channels except the roll rate and pitch rate responses which still shows good agreement.

(a) A-Matrix

	"real" value	Identified value
X_u	-0.1257	-0.1343
Y_v	-0.4247	-0.4237
L_u	-0.1677	-0.2028
L_v	0.0870	0.0790
L_a	36.7050	67.0926
L_b	161.1087	157.7030
M_u	-0.0823	-0.1186
M_v	-0.0518	-0.0614
M_a	63.5763	85.1978
M_b	-19.4931	-14.5734
τ_a	0.29	0.2849
A_b	0.8287	0.5139
B_a	0.3611	0.0936
Z_a	0	fixed to 0
Z_b	9.6401	0
Z_w	-0.7598	-0.7674
Z_r	8.4231	9.7000
N_p	-1.3300	-0.0909
N_w	0.0566	0.0854
N_r	-5.5105	-4.1457
N_{rf}	-44.8734	-
K_r	1.8157	1.5395
K_{rf}	-11.0210	-

(b) B-Matrix

	"real" value	Identified value
A_{lat}	-0.8417	-0.8565
A_{lon}	-2.8231	-2.8672
B_{lat}	2.4090	2.5012
B_{lon}	-0.3511	-0.1265
Z_{col}	-70.504	-63.511
N_{col}	23.6260	22.0576
N_{ped}	44.8734	38.4659

TABLE I
PARAMETER IDENTIFICATION

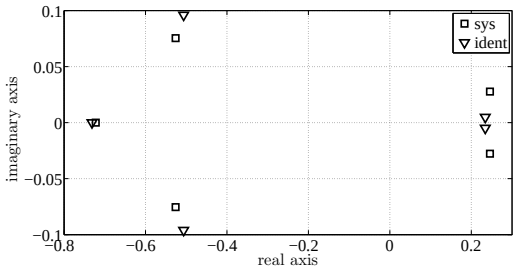

Fig. 7. Enlarged View of selected zone in Fig. 6.

VI. RESULTS FROM REAL FLIGHT DATA

The proposed system identification procedure was applied to the identification of a 60 size Hirobo "Eagle" helicopter (Fig.11) that was used for autonomous flight testing at UNSW@ADFA [5]. Several segments of the real flight data were selected to perform the time-domain grey-box system identification.

The directional velocities in x, y and z direction (u, v and w) are shown in Fig. 12. As the flight was in the hover mode and changes in velocities were small, the accuracy of the predicted velocities is limited. Apart from a slight prediction error in v, the over all results show very good agreement.

The roll rate (p), pitch rate (q), and yaw rate (r) are shown in Fig. 13. All three channels show very good agreement with real data in low frequency range where the hover dynamics is dominant.

The roll angle (Φ) and pitch angle (Θ) are in Fig. 14. Taking into account the small angle changes (±0.2rad) in the hover flight, the performance is very satisfactory.

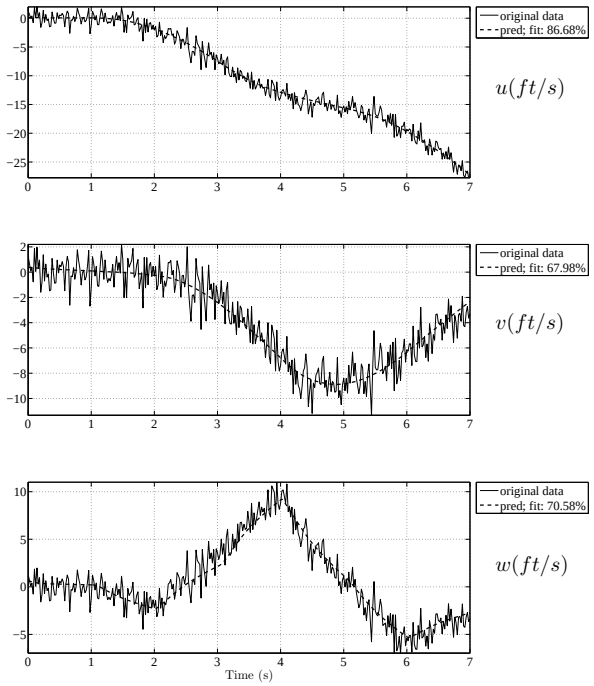

Fig. 8. Prediction performance (1).

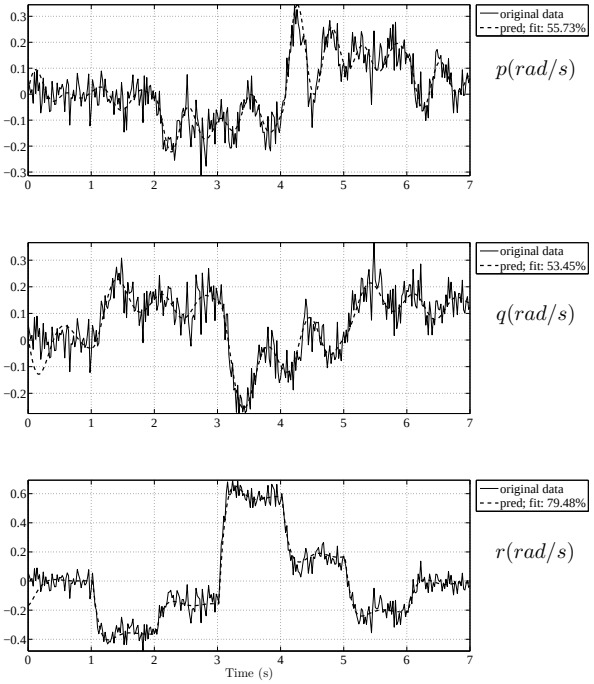

Fig. 9. Prediction performance (2).

Due to the limitation of the model structure itself, the identified model is not capable to capture the high frequency dynamics contained in the real data. But for our future control design that will enable a stable flight near hover condition, the bandwidth of the model is fairly enough.

The identified parameters are given in table II.

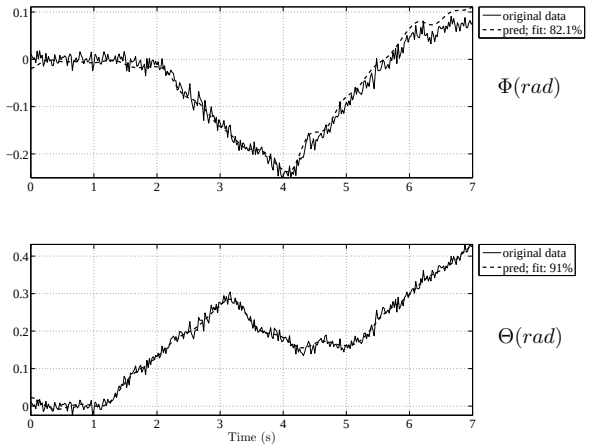

Fig. 10. Prediction performance (3).

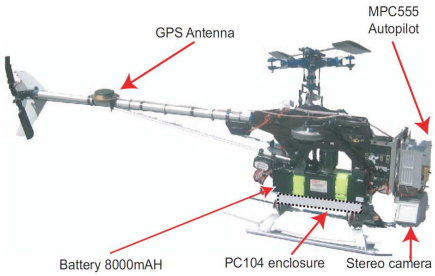

Fig. 11. The platform-Eagle [5].

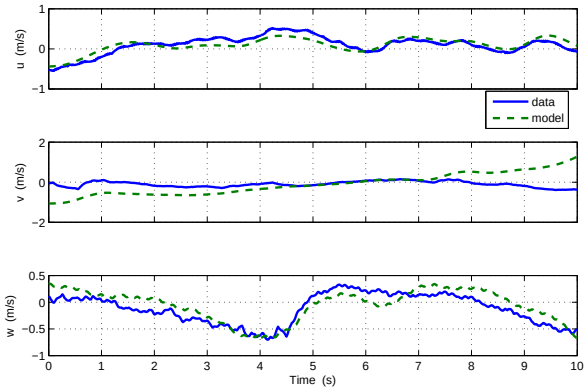

Fig. 12. Validation (1).

VII. Conclusion

A time domain grey-box system identification procedure suitable for scale-model helicopters operating in hover and near hover condition has been described. Thanks to the sign constraints added to the OEM method, the approach does not need cumbersome first-principle modeling to obtain suitable initial values. The partitioning steps of the system identification has also been described in detail through an example. In this example it has been shown that the original parameters used to generate the data set has been successfully identified through the partitioned identification method. It has

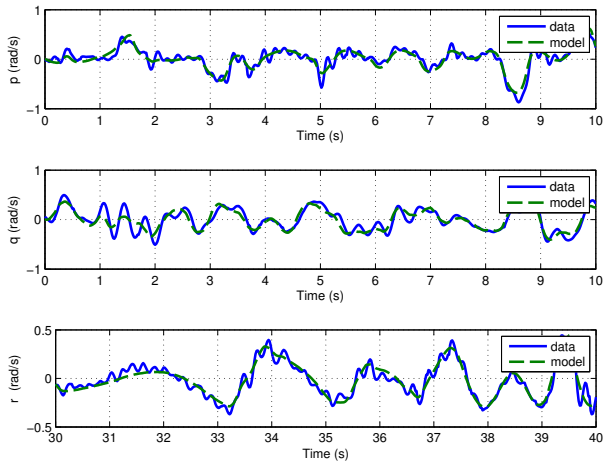

Fig. 13. Validation (2).

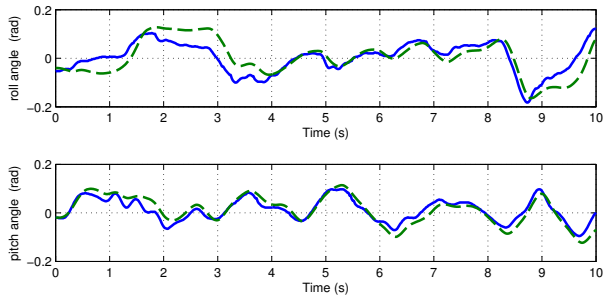

Fig. 14. Validation (3).

been shown further using the real flight data that the identified model can predict the flight performance successfully, thereby validating the proposed identification procedure in a real application.

ACKNOWLEDGEMENT

The authors would like to thank Dr. Matthew Garratt of the Australian Defence Force Academy in Canberra, Australia for providing the real flight data of the Eagle helicopter so that the validation of the system identification method could be carried out with real flight data.

(a) A-Matrix

	mean	std. error
X_u	-2.7594	0.1746
Y_v	-0.2345	0.0413
L_u	-13.308	0.8248
L_v	0.3329	0.2068
L_a	36.688	10.631
L_b	331.24	13.015
M_u	-6.2403	0.7164
M_v	0.3927	0.1344
M_a	199.36	7.8038
M_b	-41.970	10.740
τ_a	0.1064	0.0063
A_b	-6.7924	1.1007
B_a	-1.7674	0.4469
Z_a	24.106	7.1266
Z_b	35.511	4.7646
Z_w	-1.0540	0.0699
Z_r	2.1154	0.1550
N_p	0.3214	0.2523
N_w	0.2697	0.2297
N_r	-6.1107	1.37
N_{rf}	-7.4847	-
K_r	7.2914	0.5673
K_{rf}	-12.2214	-

(b) B-Matrix

	mean	std. error
A_{lat}	-0.0560	0.0074
A_{lon}	-0.4556	-0.0092
B_{lat}	0.4228	0.0059
B_{lon}	-0.2322	0.0062
Z_{col}	-7.0887	0.2397
N_{col}	2.0274	0.6639
N_{ped}	7.4847	0.8871

TABLE II
IDENTIFIED PARAMETERS FOR EAGLE RUAV

REFERENCES

[1] S. K. Kim and D. M. Tilbury, "Mathematical modeling and experimental identification of an unmanned helicopter robot with flybar dynamics," *J. Robot. Syst.*, vol. 21, no. 3, pp. 95–116, 2004.

[2] H. Shim, "Hierarchical flight control system synthesis for rotorcraft-based unmanned aerial vehicles," Ph.D. dissertation, UNIVERSITY OF CALIFORNIA, BERKELEY, 2000.

[3] G. Cai, B. M. Chen, K. Peng, M. Dong, and T. H. Lee, "Modeling and control system design for a uav helicopter," in *Proc. 14th Mediterranean Conf. Control and Automation MED '06*, 2006, pp. 1–6.

[4] K. Peng, G. Cai, B. M. Chen, M. Dong, K. Y. Lum, and T. H. Lee, "Design and implementation of an autonomous flight control law for a uav helicopter," *Automatica*, vol. 45, no. 10, pp. 2333 – 2338, 2009. [Online]. Available: http://www.sciencedirect.com/science/article/B6V21-4WVCT1V-7/2/181b4c58bb95448daab2a1bedd587084

[5] M. Garratt, B. Ahmed, and H. R. Pota, "Platform enhancements and system identification for control of an unmanned helicopter," in *Proc. 9th Int. Conf. Control, Automation, Robotics and Vision ICARCV '06*, 2006, pp. 1–6.

[6] L. Ljung, *System Identification Toolbox User's Guide*. The Math Works, Inc, 2003.

[7] M. B. Tischler and R. K. Remple, *Aircraft and Rotorcraft System Identification: Engineering Methods with Flight Test Examples*. American Institute of Aeronautics and Astronautics, 2006.

[8] B. Mettler, M. B. Tischler, and T. Kanade, "System identification of small-size unmanned helicopter dynamics," in *American Helicopter Society 55th Forum, Montreal, Quebec, Canada*, 1999.

[9] B. Mettler, *Identification Modeling and Characteristics of Miniature Rotorcraft*. Kluwer Academic Publishers, 2003.

[10] B. Mettler, M. B. Tischler, and T. Kanade, "System identification modeling of a small-scale unmanned rotorcraft for flight control design," *Journal of the American Helicopter Society*, vol. 47, pp. 50 –63, 2002.

[11] S. Lorenz and G. Chowdhary, "Non-linear model identification for a miniature rotorcraft preliminary results," in *61st Annual Forum Proceedings - AHS International*, vol. 2, 2005, pp. 1647–1660.

[12] S. Bhandari, "Flight validated high-order models of uav helicopter dynamics in hover and forward flight using analytical and parameter identification techniques," 2007.

[13] A. Budiyono, K. J. Yoon, and F. D. Daniel, "Integrated identification modeling of rotorcraft-based unmanned aerial vehicle," in *Proc. 17th Mediterranean Conf. Control and Automation MED '09*, 2009, pp. 898–903.

[14] V. Klein and E. A. Morelli, *Aircraft System Identification: Theory and Practice*. AIAA, 2006.

[15] R. Jategaonkar, *Flight vehicle system identification: a time domain methodology*. American Institute of Aeronautics and Astronautics, 2006.

[16] L. Ljung, *System identification : theory for the user*, 2nd ed. Upper Saddle River, NJ : Prentice Hall PTR, 1999.

[17] E. A. Morelli, "System identification programs for aircraft (sidpac)," in *AIAA Atmospheric Flight Mechanics Conference*, 2002.

[18] G. Cai, B. M. Chen, X. Dong, and T. H. Lee, "Design and implementation of a robust and nonlinear flight control system for an unmanned helicopter," *Mechatronics*, vol. 21, no. 5, pp. 803 – 820, 2011, special Issue on Development of Autonomous Unmanned Aerial Vehicles. [Online]. Available: http://www.sciencedirect.com/science/article/pii/S0957415811000262

[19] J. Grauer, J. Conroy, J. H. Jr., J. Humbert, and D. Pines, "System identification of a miniature helicopter," *Journal of Aircraft*, vol. vol.46 no.4, pp. 1260–1269, 2009.